Published Online: 2026 February 11 **Research Article**

Development and Optimization of Dissolvable Polymeric Microneedle Patch for Transdermal Delivery of Lawsone

Marzieh Sajadi Bami [1], Shayan Fakhraei Lahij [2], Hamid Mobedi [3], Mehrdad Hamidi [4], Reza Vahidi [5], Payam Khazaeli [6,*]

[1] Department of Pharmaceutics, Faculty of Pharmacy, Kerman University of Medical Sciences, Kerman, Iran
[2] Department of Bioengineering, Biopharmaceutical Research Laboratory, Hanyang University, Seoul, South Korea
[3] Department of Novel Drug Delivery Systems, Iran Polymer and Petrochemical Institute, Tehran, Iran
[4] Department of Pharmaceutics, School of Pharmacy, Zanjan University of Medical Sciences, Zanjan, Iran
[5] Research Center for Hydatid Diseases in Iran, Kerman University of Medical Sciences, Kerman, Iran
[6] Pharmaceutics Research Center, Institute of Pharmaceutical Sciences, Kerman University of Medical Sciences, Kerman, Iran

[*] ***Corresponding Author:*** Pharmaceutics Research Center, Institute of Pharmaceutical Sciences, Kerman University of Medical Sciences, Kerman, Iran Email: ppkhazaeli@gmail.com

Received: 31 December, 2025; **Revised:** 1 February, 2026; **Accepted:** 2 February, 2026

Abstract

Background: Transdermal drug delivery by means of polymeric microneedles (PMNs) offers the advantage of overcoming some of the disadvantages of oral medication, such as first-pass metabolism, through painless, controlled drug release. Lawsone, isolated from *Lawsonia inermis*, exhibits reported antioxidant, anti-inflammatory, antimicrobial, and antitumor properties, suggesting its use as a promising candidate for topical application.

Objectives: Fabrication and optimization of hyaluronic acid-carboxymethylcellulose (HA-CMC) PMNs loaded with lawsone with respect to enhancing transdermal delivery and understanding release and physicochemical characteristics.

Methods: Hyaluronic acid-carboxymethylcellulose-lawsone patches were prepared by micromolding. The Box-Behnken design approach was then utilized to identify the appropriate concentrations of carboxymethylcellulose (CMC) (0.15% to 0.35% w/w), hyaluronic acid (HA) (0.01% to 0.09% w/w), and polyethylene glycol 400 (PEG 400) (0.5% to 1.5% w/w), all of which are dependent on drug release after 90 minutes. Morphological examination was conducted using light and scanning electron microscopy (SEM). The levels of transepidermal water loss (TEWL), drug content, insertion rate, mechanical properties, and release of the patches were assessed.

Results: The optimized formulation showed a cumulative release of 59.63% in 90 min, following Higuchi release kinetics. Polymeric microneedles showed uniform morphology, a failure force of 0.48 N, full penetration of 375 µm, and reversible changes in TEWL.

Conclusions: Hyaluronic acid-carboxymethylcellulose PMNs offer a promising formulation strategy for the transdermal delivery of lawsone. This preliminary study establishes a biocompatible platform with potential for future development towards anti-inflammatory and antitumor therapies, pending further in vivo validation.

Keywords: Polymeric Microneedle, Optimization, Lawsone, Transdermal Delivery

1. Background

Transdermal drug delivery has gained significant attention as a major modality of contemporary pharmacotherapy for the delivery of therapeutics across the skin surface to produce systemic effects while circumventing the disadvantages of oral drug dosing, including hepatic first-pass metabolism and gastrointestinal instability (1, 2). This approach promotes patient adherence through painless and self-administered systems capable of controlled and sustained release and is particularly advantageous for chronic therapies, such as opioid replacement or pain management (3, 4). However, the stratum corneum (10 -

How to Cite: Sajadi Bami M, Fakhraei Lahij S, Mobedi H, Hamidi M, Vahidi R, et al. Development and Optimization of Dissolvable Polymeric Microneedle Patch for Transdermal Delivery of Lawsone. Jundishapur J Nat Pharm Prod. 2026;21(1):e169497. doi: https://doi.org/10.5812/jjnpp-169497

20 µm thick) is a lipophilic barrier that severely limits the permeation of hydrophilic or high-molecular-weight compounds (> 500 Da), thus confining transdermal therapeutics to only a very limited number of lipophilic small molecules (5-9). Microneedle (MN) technology provides a solution to this issue by creating micron-sized needles that increase permeability by 100 to 10,000 times, combining the ease of a patch with the precision of an injection without triggering pain or deep tissue injury (10, 11). Microneedles offer advantages over hypodermic needles by minimizing tissue damage and pain during drug delivery. Dissolving, solid, coated, and hollow MNs have emerged as invasive drug delivery options (8). Polymeric microneedles (PMNs) are also biocompatible, degradable alternatives to inorganic types (such as silicon or metal), which are prone to brittleness and toxicity issues. Polymeric MNs, 25-2000 µm long, made up of polymers polyvinyl alcohol (PVA), carboxymethyl cellulose (CMC), hyaluronic acid (HA), polyvinylpyrrolidone (PVP), or poly (ethylene glycol) diacrylate (PEGDA), penetrate the stratum corneum layers to target living layers of epidermis or dermis for immune or vascular areas (12, 13). Following ISO 10993 standards, they are gentle on skin, ensuring minimum inflammation and degradation by themselves (14). The versatility of PMNs to encapsulate biologics without denaturation and mechanical properties that withstand skin viscoelastic forces (15).

PMNs are mechanism-engineered to fit release rates for various cargoes. Dissolvable PMNs, processed from soluble HA, PVA, or PVP, disintegrate via interstitial fluid for rapid or controlled bulks for vaccine or pain relievers (16-18). Swelling-type PMNs, analogous to chitosan hydrogel, hydrate to sustain diffusion rates for days, maintaining large biomolecule structure. Biodegradable PMNs via PLGA hydrolyze for sustained release, also improving patient adherence for chronic treatment (16, 18). Coated PMNs utilize shear-off strips for rapid initiation, together with hollow PMNs facilitating infusion or “poke-and-flow” treatment (19, 20). Therapeutic PMNs are so-called for containing integrated responsive functions, including pH-sensitive coatings or nanoparticles for theranostic functions (19). Polymeric microneedles are micromolded using “legacy” technology from polydimethylsiloxane (PDMS) to cast polymer solutions under vacuum to create high-density needles (21, 22).

Lawsone, chemically called 2-hydroxy-1,4-naphthoquinone, is mainly obtained from *Lawsonia inermis*, a plant ubiquitous to North Africa, the Middle East, and South Asia. *Lawsonia inermis* is locally known as Henna, Madurang, Mendi, Manghati, Goranti, and Madayantika; it is one of the most common families of naphthoquinone dyes (23). Lawsone was first isolated in the 1950s from the leaves of the henna plant and is present at 0.5 - 1.5%. Its synthesis occurs via the phenylpropanoid pathway in the plant. Henna is a brown-green powder utilized in cosmetics. It has been extensively used not only in hair coloring products but also as dyes in textiles for coloring of cloth materials like silk, wool, and leather since 1400 BC in various parts of the world. A naturally occurring organic compound also called hennotannic acid, obtained mainly from *L. inermis* (Henna) (24). It is a potential drug-like molecule with unique chemical and biological characteristics. Traditionally, henna is used in hair and skin coloring and is also a medicinal herb for various diseases. It is also widely used as a starting material for the synthesis of various drug molecules. Literature reports indicate the chemistry, biosynthesis, physical, and biological properties of lawsone. The results showed that lawsone has potential antioxidant, anti-inflammatory, antimicrobial, and antitumor properties. It also induces cell cycle inhibition and programmed cell death in cancer, making it a potential chemotherapeutic agent. Additionally, inhibition of pro-inflammatory cytokine production makes it an essential treatment for inflammatory diseases. Exploration of its biosynthetic pathway can pave the way for its development into targets for new drug development (23, 25, 26).

2. Objectives

In this project, polymer MNs of HA and CMC containing lawsone were prepared and optimized as a potential transdermal drug delivery system. Various formulations of MN patches containing lawsone were prepared and optimized using Design Expert software based on the rate of lawsone release. The physicochemical properties of the optimized patch were investigated in a laboratory environment.

3. Methods

3.1. Fabrication of Stainless-Steel Master Mold

A high-aspect-ratio MN array template, suitable for replicating dissolvable PMNs, was fabricated in stainless steel using micro-electro-mechanical systems (MEMS) processes (27). Photolithography was used to pattern a silicon wafer and define conical MN geometries: Height 600 - 800 µm, base diameter 200 - 300 µm, aspect ratio 3 - 4, inter-needle spacing 500 µm. Sharp-tipped structures were formed by DRIE of the pattern, followed by the electroplating of a thin layer of stainless steel for durability and corrosion resistance. The master mold

consisted of an 11 × 11 array (121 MNs in total) on a 1 cm^2 base.

3.2. Polydimethylsiloxane Mold

Negative molds of PDMS were prepared by casting PDMS prepolymer (Sylgard 184, Dow Corning) over the stainless-steel master mold (28). The PDMS mixture (10:1 base-to-curing agent ratio by weight) was first degassed under vacuum for 30 min to remove air bubbles and was then poured onto the master to a thickness of 5 mm. The assembly was cured at 60°C for 4 h in a convection oven, ensuring conformal replication of the MN features with high fidelity (replication error < 2%). After curing, the PDMS mold was gently peeled from the master and then inspected for defects by optical microscopy. The mold was then treated with trichloro(1H,1H,2H,2H-perfluorooctyl)silane vapor for 1 h to render the surface hydrophobic and thus provide for easy demolding of PMNs. The flexible nature of the resulting PDMS mold supported sharp tip geometries and was reusable for more than 50 casting cycles, allowing for scalable production of PMNs.

3.3. Fabrication of Polymeric Microneedles

PMN patches were fabricated via micromolding using the PDMS mold and a blend of HA (molecular weight 1 - 2 MDa) and sodium carboxymethyl cellulose (CMC, degree of substitution 0.7 - 0.9) as the matrix polymers, loaded with lawsone (2-hydroxy-1,4-naphthoquinone) as the model drug for transdermal delivery (29, 30). HA and CMC were wetted in polyethylene glycol 400 (PEG 400) and dissolved in deionized water (pH 6.5 - 7.0) at 40 - 50°C to form a viscous solution, then lawsone was added. The mixture was stirred for 2 h, degassed, and cast into the PDMS mold using a vacuum-assisted filling technique to ensure complete penetration of cavities (applied vacuum: 0.5 bar for 10 min). Excess solution was removed by centrifugation (4000 rpm, 15 min), and the mold was dried at 37°C for 72 h in a humidity-controlled chamber (40 - 50% RH) to form solid, dissolvable PMNs. Demolded patches (1 cm^2, 121 needles) were stored in desiccated conditions.

3.4. Optimization of Polymeric Microneedles

To identify the most important levels of factors that potentially affect the PMNs, an experimental design of Box Behnken was used (Design Expert 12.0.0 software) (31). The selected factors were CMC concentration, HA concentration, and PEG concentration. The specified codes for each factor and its levels are presented in Table 1. Drug release is one of the important factors in the effectiveness of various drug delivery systems, including MNs. Therefore, the percentage of release at the time of reaching the plateau was considered as the response for optimization (32, 33).

3.5. Morphology Characterization

Needle geometry assessments, like MN tip radius and length, are very important. Scanning electron microscopy (SEM) and optical microscopy are performed to provide a dimensional evaluation (34). Dried PMNs were gold-sputtered (10 nm thickness) and imaged at 5 - 15 kV acceleration voltage in low-vacuum mode to visualize tip sharpness, base uniformity, and surface topography at magnifications of 50 - 5000.

3.6. Determination of the Mechanical Properties of Microneedles

Microneedles should be sharp, slender, and strong to achieve appropriate permeation with no breakage. Insertion force/depth and failure force are important mechanical properties, measured using techniques of dye marking and force-displacement testing (35). A high insertion-to-failure force ratio (safety factor) is preferred. Microneedle integrity and insertion force, regarding the safety of designs, is evaluated by compressing on a Texture Analyzer. Pre- and post-compression, MN array heights are measured. The arrays are mounted on a steel platform and subjected to a predefined force for 30 seconds. The MN heights were measured post-compression under a microscope. Height reduction (%) vs force can be plotted from direct measurements.

3.7. Insertion Test

Eight layers of Parafilm™ (PF) film (2.0 cm × 2.0 cm, ca. 1000 µm thick) were stacked, and a MN patch was applied with 10 N of force for 2 min (36, 37). Following the removal of the MN patch, the number of PF layers pierced, and surface micropores were quantified [tests were performed in triplicate (n = 3)]. Penetration rate was then calculated as the following equation:

$$Penetration\ rate = \frac{X}{Y} \times 100$$

where X = number of surface pores remaining, and Y = total number of needles.

3.8. Transepidermal Water Loss

Transepidermal water loss (TEWL) was measured using a Tewameter to assess skin barrier integrity post-

Table 1. Factors and Levels Are Used in the Design of an Experiment for Optimizing Polymeric Microneedles

Factor (Concentration)	Symbol	Unit	Level		
			Low	M	High
CMC	A	(%w/w)	0.15	0.20	0.35
HA	B	(%w/w)	0.01	0.05	0.09
PEG 400	C	(%w/w)	0.50	1.00	1.50

Abbreviations: HA, hyaluronic acid; PEG 400, polyethylene glycol 400.

PMN insertion (38-40). The studies utilized rat skin obtained from animals sacrificed for other purposes approved by the Institutional Animal Care and Use Committee. All procedures were in accordance with the guidelines of the Kerman University of Medical Sciences Animal Ethics Committee (approval code: IR.KMU.REC.1400.567). Rat skin samples (n = 6) were equilibrated at 32°C and 50% RH for 30 min, with baseline TEWL recorded. Optimized PMNs were inserted as in Section 3.7, and TEWL was monitored at 0, 1, 3, 6, and 24 h post-removal. Temporary increases (20 - 30% above baseline at 1 h) indicated microchannel formation without permanent damage, returning to < 10% elevation by 24 h, confirming reversibility and minimal irritation for lawsone delivery.

3.9. Drug Content Determination

Microneedle arrays were carefully taken out from the molds and placed in a 20 mL vial to be dissolved in 10 mL PBS by magnetic stirring at 4000 rpm for 30 min. After that, centrifugation was done at 5000 rpm for 10 min to remove any aggregated particles (41). A 100 µL of the supernatant was serially diluted to make its absorbance value readable via UV-visible spectroscopy and defined by a calibration curve range.

3.10. UV-Visible Quantification

To determine the maximum absorption wavelength of lawsone, solutions of 40, 80, and 200 µg/ml in a water and ethanol mixture (50:50) were first prepared. A spectrophotometer was then used to scan the wavelength range of 200 - 650 nm, with the maximum absorption wavelength identified based on the observed peak (42). To prepare the initial stock solution, 10 mg of the substance was weighed and then diluted with 50% ethanol to a final volume of 10 mL, resulting in a stock solution with a concentration of 1000 µg/mL. Subsequently, to create a secondary stock solution, 1 mL was taken from the primary stock and diluted to 10 mL with 50% ethanol, yielding a secondary stock concentration of 100 µg/mL. Standard working solutions were then prepared at concentrations of 2, 4, 5, 8, and 10 µg/mL, and the absorption of each was measured at the maximum absorption wavelength using UV-visible spectroscopy. To improve the accuracy of constructing and reading the absorption of working standards, the process was repeated three times. The standard curve was generated using Microsoft Excel software, and its equation was determined for future reference. Least squares linear regression and correlation analysis were conducted on the obtained calibration curves. The limit of detection (LOD) and limit of quantification (LOQ) for each method were also established.

3.11. Dissolution Test

In an attempt to model the process by which MNs prick the wet surface of the skin, the gelatin model system was opted for. In this respect, a gelatin film was developed, which had similar mechanical values (Young's modulus, etc.) to those of the stratum corneum layer of the epidermal surface of the skin. This film material was made from a gelatin solution that had a concentration of 12.5% w/v in water at 37°C. A fixed quantity of gelatin powder was mixed in 10 ml of distilled water at 40°C to get a solution that is completely transparent. This solution was poured into a 4 × 10 cm mold. Freezing the solution for at least 8 hours in the refrigerator led to the formation of a semisolid hydrogel, which had a similar consistency to that of the skin, particularly the epidermal layer, which has a relatively high water content (43).

3.12. Ex Vivo Drug Release

To determine the skin permeation kinetics of drug-encapsulated PMNs, they were applied to rat skin mounted on Franz cells over periods that reached the plateau (44). To determine the skin permeation kinetics, drug-encapsulated PMNs were applied to full-thickness rat abdominal skin, mounted on Franz-type diffusion cells (Receptor volume: 30 mL). The receptor compartment was filled with phosphate-buffered saline

(PBS, pH 7.4) maintained at 32 ± 0.5°C under continuous magnetic stirring. Samples (1 mL) were withdrawn from the receptor compartment at predetermined time intervals (15, 30, 45, 60, 90, 120 min) and replaced with an equal volume of fresh pre-warmed PBS. The concentration of lawsone in the samples was quantified using the validated UV-visible method described in Section 3.10. Cumulative drug release was calculated and plotted against time.

3.13. Statistical Analysis

For the Design of Experiments, analysis of variance (ANOVA) was performed using Design Expert software. For other experiments, data are presented as mean ± standard deviation (SD). The sample size (n) for each experiment is reported in the respective method or result section and was chosen based on common practices in preliminary formulation studies to assess variability and trends.

4. Results

The results obtained in this project will be mentioned below.

4.1. Fabrication and Optimization of Polymeric Microneedles

Polydimethylsiloxane molds were made in such a way that the patch produced from them had an 11 × 11 arrangement and an area of 1 cm^2. Based on the method (Section 3.3) and Table 1, 15 formulations of MN skin patches were prepared. The center points (F13-F15) were replicates (n = 3) for estimating pure error. These formulations were evaluated for the percentage of lawsone released upon reaching the plateau (90 minutes), and the release percentages were input into the software (Table 2). Following optimization, the proposed model was refined using Design Expert software along with one-way analysis of variance data. The results are displayed in Appendix 1 in Supplementary File. The proposed model yielded a P-value of less than 0.05, indicating its validity. Furthermore, the lack of fit was greater than 0.05, which is favorable for the proposed model. The values of R^2 and adjusted R^2 are 0.9998 and 0.9994, respectively, which indicate the linearity of the proposed model. The formula suggested by the software for optimization is provided below.

Response = +23.33 -13.60 * C -2.22 * A * B +9.17 * A * C -4.05 * B * C +0.83 * A^2 +9.76 * B^2 +6.86 * C^2 -5.87 * A^2 * B +9.17 * A^2 * C -4.73 * A * B^2

A: CMC concentration, B: HA concentration, C: PEG 400 concentration

Figure 1 illustrates the relationship between the model's predicted data and the actual data, and Figure 2 demonstrates the impact of various factors on the percentage of release. To validate the predictive capability of the model and address concerns of overfitting, two random checkpoint formulations (FV1 and FV2, Table 3), which were not part of the original experimental design matrix, were prepared alongside the software's optimal formula, and their release percentages were calculated and shown in Table 3. The results confirm a validated formula for optimizing the patch formulation based on the release percentage. The close agreement between predicted and actual values, with the latter falling within the 95% confidence intervals, confirms the model's robustness and predictive power for interpolation within the design space. The level factors of the optimal formula (FO) are presented in Appendix 3 in Supplementary File.

4.2. Morphology Characterization

Light and electron microscopes were utilized to investigate the morphology of the PMNs. Figures 3A and Figures 3B present the light microscope images of the PMNs, illustrating the uniformity of the MN shafts, their integrity, and their orderly arrangement. Figures 3C and Figures 3D display the electron microscope images of the MNs, highlighting their pyramidal shape, consistent arrangement, and well-defined tips.

4.3. Mechanical Properties of Microneedles

The general force-displacement plot of PMN's skin penetration is shown in Appendix 4 in Supplementary File. The change in slope indicates the point of needle breakage (this is approximately 0.48 N). The test was repeated on five separate patches (n = 5).

4.4. Insertion Test and Transepidermal Water Loss

Parafilm insertion testing showed 100% permeability up to the third layer, with no permeability observed at the sixth layer. The results of this test are presented in Appendix 2 in Supplementary File.

The results of the TEWL study in the control group and the group to which the PMNs were inserted on the skin of rats are presented in Figure 4. The results show a significant decrease in TEWL 6 hours after PMN application.

4.5. UV-Visible Quantification

The UV absorption of lawsone was investigated in the range of 200 to 400 nm (Appendix 5A in Supplementary File), and the wavelength of 270 nm was determined as

Table 2. Experimental Design and Formulation Composition

Formulation	Value of Independent Factor [a]			Released Lawsone (%)
	A	B	C	
F1	0.15	0.01	1.00	42.30
F2	0.35	0.01	1.00	37.30
F3	0.15	0.09	1.00	35.00
F4	0.35	0.09	1.00	21.10
F5	0.15	0.05	0.50	44.60
F6	0.35	0.05	0.50	26.30
F7	0.15	0.05	1.50	17.40
F8	0.35	0.05	1.50	35.80
F9	0.25	0.01	0.50	49.50
F10	0.25	0.09	0.50	57.60
F11	0.25	0.01	1.50	30.40
F12	0.25	0.09	1.50	22.30
F13	0.25	0.05	1.00	23.20
F14	0.25	0.05	1.00	23.80
F15	0.25	0.05	1.00	23.00

[a] A, CMC concentration; B, HA concentration; C, PEG 400 concentration.

the wavelength of maximum absorption. The standard curve for determining the concentration of lawsone was drawn using Microsoft Office Excel software and is shown in Appendix 5B in Supplementary File. The LOD and LOQ values were obtained as 0.54 and 1.80 μg/mL, respectively.

4.6. Drug Content Determination

Based on the optimal formula from previous sections, 5 MNs were tested, and their drug content was quantified (Table 4).

4.7. Dissolution Test

To simulate the process of MN unfolding in the moist environment of the skin, a gelatin model was employed. Imaging was conducted at time zero, one, three, and five minutes following exposure to the gelatin block (Appendix 6 in Supplementary File). The results indicated that the MN patch can dissolve and release the drug into the skin upon contact.

4.8. Ex Vivo Drug Release

The cumulative release of all PMN formulations was investigated. The results of the release at the time of reaching the plateau are reported in Table 2. Figure 5A shows the release diagram of the optimal formulation, and Figure 5B shows the release diagram of the formulation used in validating the proposed model of Design Expert software. The percentage of release (90 min) in these two formulations was 59.63 and 39.88, respectively. The release kinetics were also investigated, and the results are presented in Table 5. Most formulations follow the Higuchi release kinetics.

5. Discussion

The work moves forward the cause of transdermal drug delivery with lawsone-loaded dissolving PMNs constituted from HA and CMC. By employing Box-Behnken design, lawsone MNs for controlled drug delivery were developed with approximately 59.63% lawsone release at 90 minutes in ex vivo experiments via the Higuchi diffusion mechanism. Higuchi's equation models drug release from a uniform matrix as a diffusion process, dependent on the square root of time and Fick's law, applicable to modified release forms like transdermal patches (17, 45). The finding indicates better penetration with least invasiveness, owing to homogeneous needle structure, sufficient strength to withstand mechanical forces, proficient insertion without damaging the skin, and temporary disruption to the skin barrier, making this formulation a promising alternative for lawsone for its therapeutic uses (46, 47).

Box-Behnken design revealed the specific influence of formulation parameters on lawsone release (48, 49). The derived model ($R^2 = 0.9998$, adjusted $R^2 = 0.9994$, $P < 0.0001$) established that increased PEG levels impede release, likely due to variations in matrix hydrophilicity and drug solubility. There was a positive interaction effect for CMC-PEG, whereas HA-PEG interaction effects

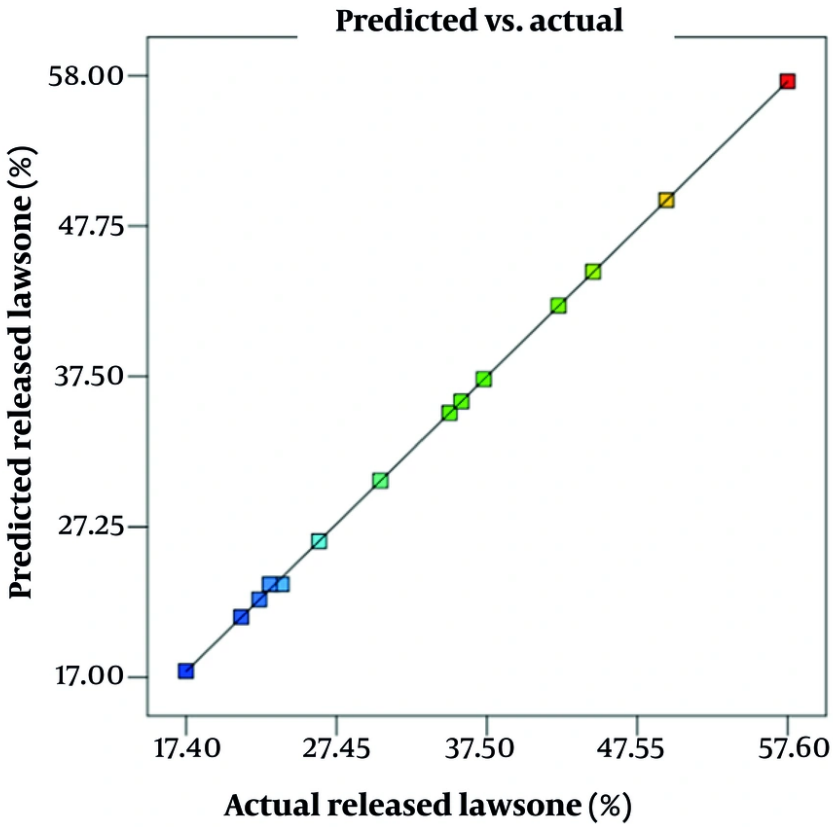

Figure 1. The predicted values by the model against actual values of released lawsone (%).

were negative, as was demonstrated in 3D Response Surface plots. In line with contemporary MN technology optimization, as witnessed in benidipine-loaded nanotransfersomes in dissolving MNs (48). In order to assess random formulation validity, validation analysis proved the forecasting ability of the proposed model by successfully keeping all released values under 95% confidence intervals, thus validating statistical design input in the field of pharmaceutics. In direct relation to transdermal technology, by considering the plateau value of release as 'response', it addressed prominent transdermal issues by striving to maintain constant drug (50).

Detailed microscopic examination indicated pyramidal MNs with tapered tips precisely arrayed in an 11 × 11 grid with a base of 1 cm^2 for accurate reproduction from the PDMS mold, with a focus on penetrating the stratum corneum. This microneedling array addressed concerns of inconsistent distribution or breakage, consistent with emerging polymer MNs launched for biocompatibility and precise transdermal delivery mechanisms (51, 52). In mechanical testing, it was found that the break force was approximately 0.48 N based on force-displacement analysis and outpaced the insertion force of typical MNs (0.1 N to 0.3 N) by a significant margin for enhanced protection against breakage. Compared to recent research studies of commercially available MN with a peak breakage force of 14 N but MNs that exhibited deformation under compression, these hyaluronic acid-carboxymethylcellulose (HA-CMC) blends exhibited excellent performance (15, 53, 54).

Insertion trials with Parafilm resulted in 100% penetration for outer layers (approximately 375 µm), with a tapered effect afterwards, reflecting targeted epidermal application with pain receptor sparing. Transepidermal water loss indicated a transient breakage with a relative increase of 20 - 30% over baseline after 1 h, reverting to less than 10% by 24 h,

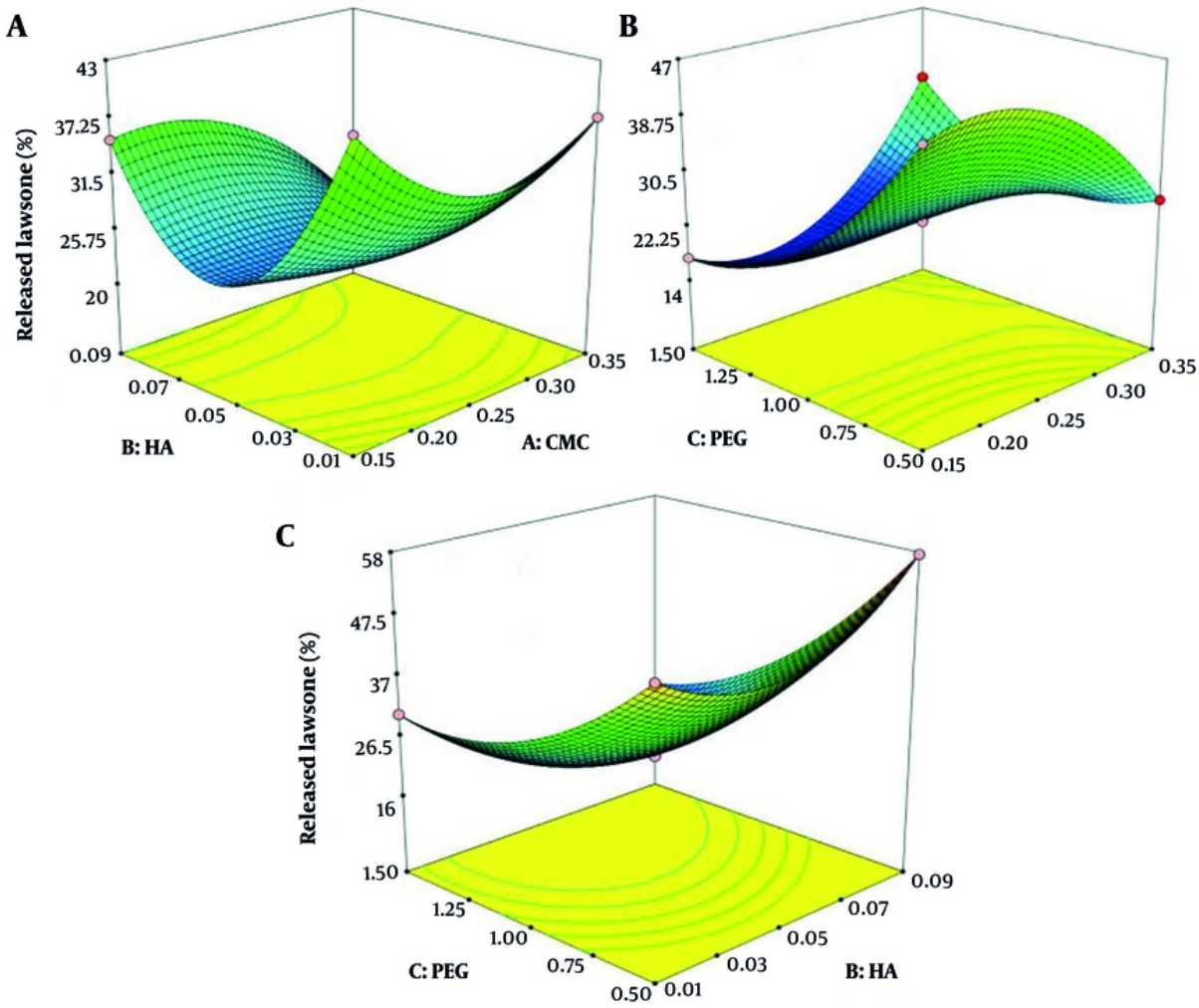

Figure 2. Three-dimensional graph of the simultaneous effect of various factors. A, CMC and HA concentration; B, PEG 400 and CMC concentration; C, PEG 400 and HA concentration.

Table 3. Model Validation Results with Two Random Formulas [a]

Formulation	CMC Concentration	HA Concentration	PEG 400 Concentration	Predicted Release (CI: 95%)	Actual Release
FV1	0.32	0.09	0.5	38.43 - 40.71	39.88
FV2	0.17	0.04	0.95	26.18 - 26.96	26.97
FO	0.24	0.09	0.5	57.66 - 59.78	59.63

Abbreviations: HA, hyaluronic acid; PEG 400, polyethylene glycol 400.

[a] Values are expressed as (%w/w).

reflecting microchannel formation with less irritation. Outcome in rat skin studies correlated with ex vivo porcine skin results, showing a partial insertion (up to 48%), depending on needle density and tip

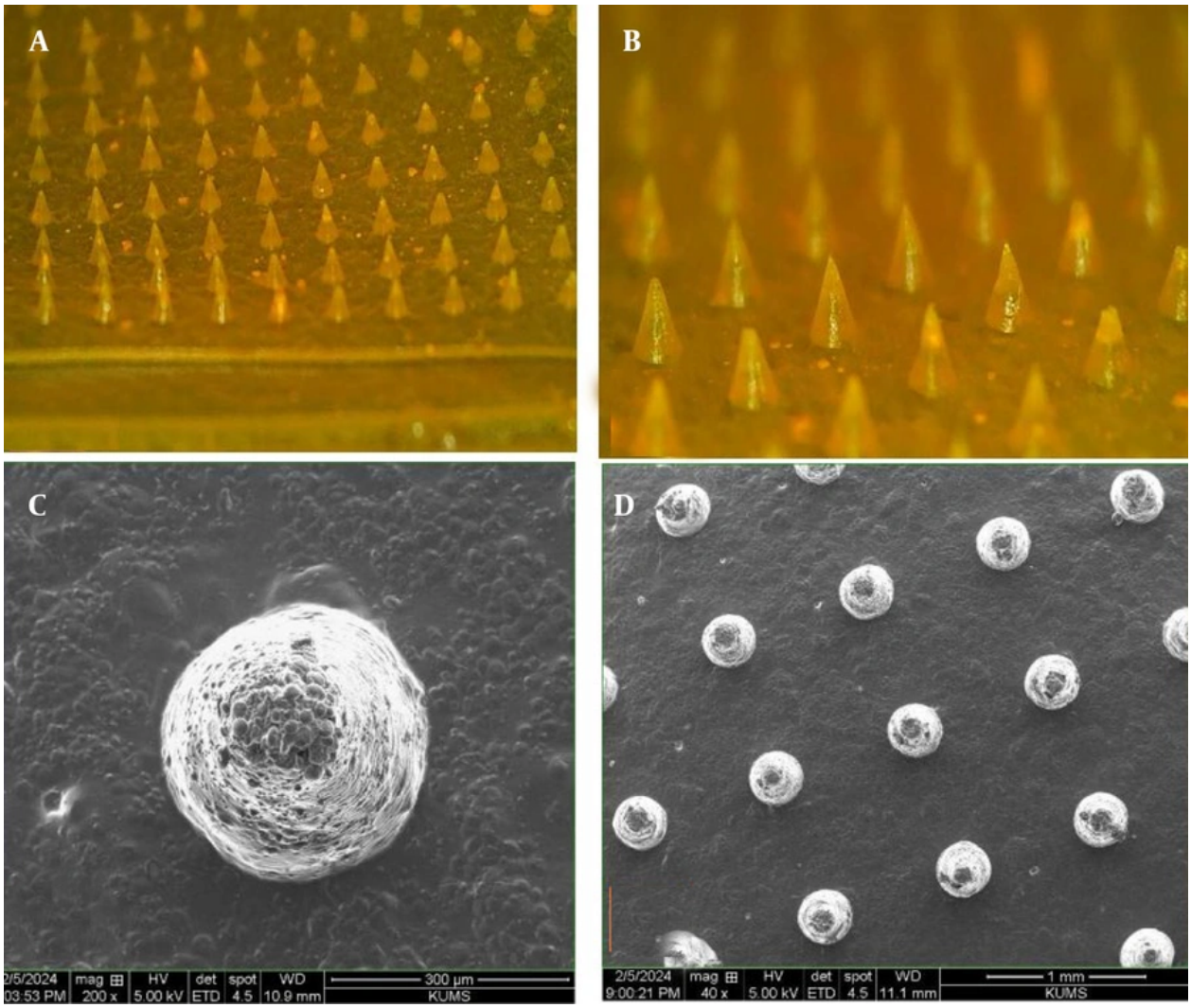

Figure 3. A and B, light microscope image of skin patch; C and D, scanning electron microscope image (scale is noted at the bottom of the image)

configuration, reflecting the patient-friendly efficacy of PMNs over conventional needles (53-55).

Average uniformity of drugs was 99.12% ± 3.73%, signifying equal distribution of lawsone and no loss of substance in fabrications. UV visibility at 270 nm (LOD 0.54 µg/mL and LOQ 1.80 µg/mL) proved efficient in ethanol-water mixtures. Gel dissolution took only 5 minutes, which is sufficient for rapid action through matrix erosion (56). Higuchi models were primarily observed ($R^2 > 0.90$ for most samples) in ex vivo release kinetics, signifying square-root time dependencies through the HA-CMC matrix (57). The optimal formula releasing 59.63% of substance in 90 minutes signifies controlled delivery rather than burst release, unlike some materials, including mixed micelle indomethacin-loaded dissolving MNs with first-order and Higuchi models for controlled delivery (58).

Lawsone encapsulation in PMNs utilizes its broad pharmacology, such as antioxidant activity through radical scavenging and enzyme induction, anti-inflammatory properties through the regulation of cytokines (e.g., TNF-α, IL-6), and possible antitumor property through apoptosis and cell cycle arrest, respectively (59). Although lawsone has been used traditionally in henna for dermatologic and hair purposes, the topical route of application may

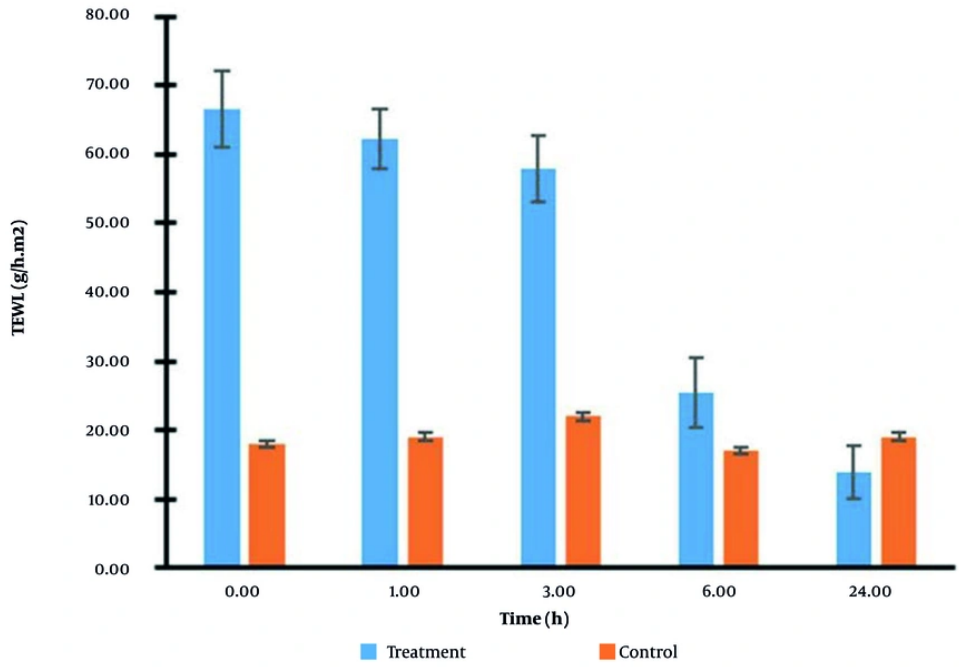

Figure 4. Transepidermal water loss (TEWL) levels in the control group and the treatment group [polymeric microneedles (PMNs) inserted skin] during 24 hours (n = 6)

Table 4. Results of Examining the Amount of Drug in the 5 Polymeric Microneedles Inserted Skin

PMN No.	Drug Content	Mean ± SD
1	98.95	99.12 ± 3.73
2	94.78	
3	103.65	
4	102.00	
5	96.25	

Abbreviation: PMN, polymeric microneedles.

overcome oral restrictions (easily eliminated) for anti-inflammatory and anticancer complementary therapies. The HA-CMC hydrogel supports the integrity of the naphthoquinone moiety of lawsone, based on the ISO 10993 standard, thereby reducing denaturation (60).

5.1. Limitations and Future Perspectives

It is important to acknowledge that this study is primarily focused on formulation development and ex vivo characterization. The absence of in vivo pharmacokinetic and pharmacodynamic data represents a key limitation in directly asserting therapeutic efficacy. This was a deliberate scope limitation for this initial proof-of-concept work, which was constrained by resources. However, the optimized parameters and promising ex vivo performance reported here provide an essential foundation for subsequent biological evaluation. Future work will prioritize in vivo studies in rodent models to evaluate the pharmacokinetic profile, anti-inflammatory efficacy in a standardized model (e.g., carrageenan-induced paw edema), and preliminary safety/toxicology of the lawsone-loaded PMNs.

5.2. Conclusions

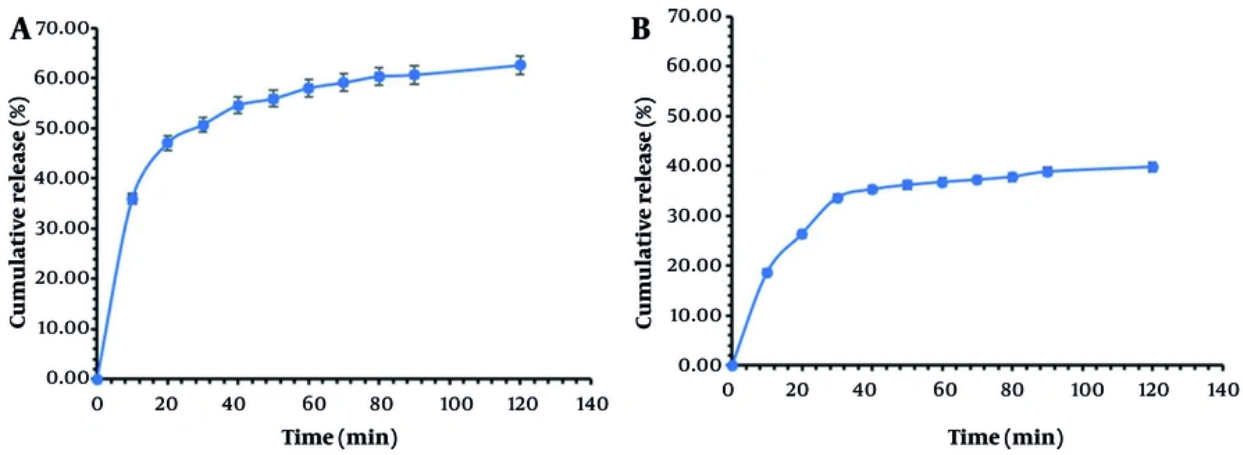

Figure 5. Cumulative release of lawsone from PMN. A, optimum formulation (Table 3); B, validation formulation (Table 3)

Table 5. Result of Ex Vivo Kinetic Release Study Profile of Polymeric Microneedles

Formulation	Zero-Order		First Order		Higuchi		Peppas			Hixon-Crowell	
	K	R^2	K	R^2	K	R^2	K	R^2	n	K	R^2
F1	0.525	0.793	0.006	0.855	4.645	0.965	0.078	0.967	0.378	0.095	0.836
F2	0.476	0.790	0.005	0.820	4.170	0.926	0.018	0.885	0.701	0.008	0.810
F3	0.456	0.696	0.005	0.719	4.013	0.876	0.022	0.806	0.647	0.008	0.712
F4	0.256	0.855	0.003	0.870	2.234	0.957	0.010	0.941	0.693	0.004	0.865
F5	0.577	0.705	0.007	0.762	5.121	0.890	0.037	0.581	0.763	0.010	0.743
F6	0.345	0.668	0.004	0.697	3.081	0.891	0.048	0.840	0.397	0.005	0.688
F7	2.111	0.876	0.002	0.890	1.834	0.970	0.009	0.960	0.665	0.003	0.886
F8	0.438	0.852	0.005	0.876	3.802	0.947	0.015	0.945	0.720	0.007	0.868
F9	0.616	0.835	0.008	0.877	5.362	0.944	0.021	0.924	0.722	0.116	0.865
F10	0.727	0.774	0.011	0.827	6.373	0.915	0.030	0.884	0.681	0.014	0.810
F11	0.390	0.763	0.005	0.790	3.434	0.927	0.024	0.879	0.586	0.006	0.780
F12	0.196	0.840	0.002	0.855	1.716	0.967	0.120	0.946	0.590	0.003	0.850
F13	0.293	0.827	0.003	0.850	2.562	0.959	0.153	0.911	0.628	0.005	0.843
F14	0.285	0.923	0.003	0.939	2.458	0.978	0.010	0.979	0.706	0.005	0.934
F15	0.301	0.689	0.003	0.708	2.687	0.899	0.035	0.866	0.439	0.005	0.702
FO	0.802	0.592	0.012	0.716	2.744	0.984	0.233	0945	0.218	0.106	0.675

This study successfully developed and optimized a dissolving PMN patch based on HA and CMC for the formulation of lawsone, a natural compound with reported bioactivity. It was observed that the stratum corneum barrier could be overcome by the optimized HA-CMC PMNs. Plant extract-based systems with a similar design signify a diffusion-controlled delivery mechanism from the polymeric matrix rather than an immediate burst release, enhanced bioactivity, thus implying the potential of polysaccharide matrices in carrying herbal actives. Additionally, these PMNs possess a high degree of biocompatibility and degradability, meeting ISO biocompatibility requirements, making them a patient-friendly alternative to injections.

Acknowledgements

This article is the result of a research project, which was carried out with the financial support of the

Kerman University of Medical Sciences (Grant No. 4000000799).

Supplementary Material

Supplementary material(s) is available here [To read supplementary materials, please refer to the journal website and open PDF/HTML].

Footnotes

AI Use Disclosure: The authors declare that no generative AI tools were used in the creation of this article.

Authors' Contribution: Study concept and design: P. Kh.; Analysis and interpretation of data: M. S., H. M., and M. H.; Drafting of the manuscript: M. S.; Critical revision of the manuscript for important intellectual content: S. F. L., M. H., and P. Kh.; Statistical analysis: M. S.; Administrative, technical, and material support: S. F. L., H. M., M. H., and P. Kh.; Study supervision: P. Kh.

Conflict of Interests Statement: The authors have no conflict of interest.

Data Availability: The dataset presented in the study is available on request from the corresponding author during submission or after publication.

Ethical Approval: This study is approved under the ethical approval code of IR.KMU.REC.1400.567.

Funding/Support: This article is the result of a research project, which was carried out with the financial support of the Kerman University of Medical Sciences (Grant No. 4000000799). (Webpage of the grant number: https://research.kmu.ac.ir/webdocument/load.action?webdocument_code=1000&masterCode=95006209)

References

1. Raeisi Estabragh MA, Sajadi Bami M, Dehghannoudeh G, Noudeh YD, Moghimipour E. Cellulose derivatives and natural gums as gelling agents for preparation of emulgel-based dosage forms: A brief review. *Int J Biol Macromol*. 2023;**241**:124538. [PubMed ID: 37085064]. https://doi.org/10.1016/j.ijbiomac.2023.124538.
2. Raeisi Estabragh MA, Pardakhty H, Pardakhty A. Preparation, Pharmaceutical Characterization, In-Vitro Release Kinetics, and Antifungal Efficacy Investigation of Fluconazole Niosomal Hydrogel. *Pharm Sci*. 2025;**31**(4):440-51. https://doi.org/10.34172/ps.025.42799.
3. Afsharipour S, Estabragh MAR, Namaki A, Ohadi M, Moshafi MH, Banat IM, et al. Preparation and Physicochemical Properties of a Thermosensitive Hydrogel-based Lipopeptide Biosurfactant. *Lett Drug Des Discov*. 2024;**21**(17):3757-64. https://doi.org/10.2174/0115701808296878240419065845.
4. Salehi T, Raeisi Estabragh MA, Salarpour S, Ohadi M, Dehghannoudeh G. Absorption enhancer approach for protein delivery by various routes of administration: a rapid review. *J Drug Target*. 2023;**31**(9):950-61. [PubMed ID: 37842966]. https://doi.org/10.1080/1061186X.2023.2271680.
5. Khazaeli P, Karamouzian M, Rohani S, Sadeghirad B, Ghalekhani N. Effects of minoxidil gel on burn wound healing in rats. *Iran J Pharm Res*. 2014;**13**(1):243-51. [PubMed ID: 24734077]. [PubMed Central ID: PMC3985251].
6. Mostafavi M, Farajzadeh S, Sharifi I, Khazaeli P, Sharifi H. Leishmanicidal effects of amphotericin B in combination with selenium loaded on niosome against Leishmania tropica. *J Parasit Dis*. 2019;**43**(2):176-85. [PubMed ID: 31263321]. [PubMed Central ID: PMC6570717]. https://doi.org/10.1007/s12639-018-1071-2.
7. Mostafavi M, Khazaeli P, Sharifi I, Farajzadeh S, Sharifi H, Keyhani A, et al. A Novel Niosomal Combination of Selenium Coupled with Glucantime against Leishmania tropica. *Korean J Parasitol*. 2019;**57**(1):1-8. [PubMed ID: 30840792]. [PubMed Central ID: PMC6409218]. https://doi.org/10.3347/kjp.2019.57.1.1.
8. Bami MS, Khazaeli P, Lahiji SF, Dehghannoudeh G, Banat IM, Ohadi M. Potential of biosurfactant as green pharmaceutical excipients for coating of microneedles: A mini review. *AIMS Microbiol*. 2024;**10**(3):596-607. [PubMed ID: 39219752]. [PubMed Central ID: PMC11362267]. https://doi.org/10.3934/microbiol.2024028.
9. Sparr E, Bjorklund S, Pham Q, Mojumdar EH, Stenqvist B, Gunnarsson M, et al. The stratum corneum barrier – From molecular scale to macroscopic properties. *Curr Opin Colloid Interface Sci*. 2023;**67**. https://doi.org/10.1016/j.cocis.2023.101725.
10. Al-Nimry SS, Daghmash RM. Three Dimensional Printing and Its Applications Focusing on Microneedles for Drug Delivery. *Pharmaceutics*. 2023;**15**(6). [PubMed ID: 37376046]. [PubMed Central ID: PMC10302545]. https://doi.org/10.3390/pharmaceutics15061597.
11. Mdanda S, Ubanako P, Kondiah PPD, Kumar P, Choonara YE. Recent Advances in Microneedle Platforms for Transdermal Drug Delivery Technologies. *Polymers*. 2021;**13**(15). [PubMed ID: 34372008]. [PubMed Central ID: PMC8348894]. https://doi.org/10.3390/polym13152405.
12. Babu MR, Vishwas S, Khursheed R, Harish V, Sravani AB, Khan F, et al. Unravelling the role of microneedles in drug delivery: Principle, perspectives, and practices. *Drug Deliv Transl Res*. 2024;**14**(6):1393-431. [PubMed ID: 38036849]. https://doi.org/10.1007/s13346-023-01475-9.
13. Wang Z, Tong S, Niu J, Cao C, Gao A, Jiao Y, et al. Microneedles: multifunctional devices for drug delivery, body fluid extraction, and bio-sensing. *Nanoscale*. 2025;**17**(2):740-73. [PubMed ID: 39606819]. https://doi.org/10.1039/d4nr03538k.
14. Thangaraju P, Varthya SB. ISO 10993: Biological Evaluation of Medical Devices. In: Shanmugam PST, Thangaraju P, Palani N, Sampath T, editors. *Medical Device Guidelines and Regulations Handbook*. Cham, Switzerland: Publisher: Springer; 2022. p. 163-87. https://doi.org/10.1007/978-3-030-91855-2_11.
15. Liu Y, Mao R, Han S, Yu Z, Xu B, Xu T. Polymeric Microneedle Drug Delivery Systems: Mechanisms of Treatment, Material Properties, and Clinical Applications-A Comprehensive Review. *Polymers*. 2024;**16**(18). [PubMed ID: 39339032]. [PubMed Central ID: PMC11434959]. https://doi.org/10.3390/polym16182568.
16. Lopez-Ramirez MA, Kupor D, Marchiori L, Soto F, Rueda R, Reynoso M, et al. Combinatorial microneedle patch with tunable release kinetics and dual fast-deep/sustained release capabilities. *J Mater Chem B*. 2021;**9**(9):2189-99. [PubMed ID: 33651048]. https://doi.org/10.1039/d1tb00141h.
17. Park JH, Allen MG, Prausnitz MR. Polymer microneedles for controlled-release drug delivery. *Pharm Res*. 2006;**23**(5):1008-19.

[PubMed ID: 16715391]. https://doi.org/10.1007/s11095-006-0028-9.

18. Chavoshi S, Rabiee M, Rafizadeh M, Rabiee N, Shamsabadi AS, Bagherzadeh M, et al. Mathematical modeling of drug release from biodegradable polymeric microneedles. *Bio-Des Manuf*. 2019;**2**(2):96-107. https://doi.org/10.1007/s42242-019-00041-y.
19. Ullah A, Khan H, Choi HJ, Kim GM. Smart Microneedles with Porous Polymer Coatings for pH-Responsive Drug Delivery. *Polymers*. 2019;**11**(11). [PubMed ID: 31703443]. [PubMed Central ID: PMC6918349]. https://doi.org/10.3390/polym11111834.
20. Kulkarni D, Gadade D, Chapaitkar N, Shelke S, Pekamwar S, Aher R, et al. Polymeric Microneedles: An Emerging Paradigm for Advanced Biomedical Applications. *Sci Pharm*. 2023;**91**(2). https://doi.org/10.3390/scipharm91020027.
21. Lamie C, Chioni AM, Garrido-Mesa N, Elshaer A. Polymeric Microneedles: Advancing Potential Through Innovative Manufacturing, Polymer Design, and Characterization Techniques. *Curr Pharm Des*. 2025;**32**(11). [PubMed ID: 40735998]. https://doi.org/10.2174/0113816128376011250706183030.
22. Juster H, van der Aar B, de Brouwer H. A review on microfabrication of thermoplastic polymer-based microneedle arrays. *Polym Engin Sci*. 2019;**59**(5):877-90. https://doi.org/10.1002/pen.25078.
23. Singh DK, Luqman S, Mathur AK. Lawsonia inermis L. – A commercially important primaeval dying and medicinal plant with diverse pharmacological activity: A review. *Ind Crops Prod*. 2015;**65**:269-86. https://doi.org/10.1016/j.indcrop.2014.11.025.
24. Abd-El-Haleem DAM. Back to nature: henna extracts from nanotech to environmental biotechnology - a review. *BioTechnologia*. 2023;**104**(4):421-34. [PubMed ID: 38213476]. [PubMed Central ID: PMC10777720]. https://doi.org/10.5114/bta.2023.132776.
25. de Franca MNF, Isidorio RG, Bonifacio JHO, Dos Santos EWP, Santos JF, Ottoni FM, et al. Anti-proliferative and pro-apoptotic activity of glycosidic derivatives of lawsone in melanoma cancer cell. *BMC Cancer*. 2021;**21**(1):662. [PubMed ID: 34078316]. [PubMed Central ID: PMC8173884]. https://doi.org/10.1186/s12885-021-08404-4.
26. Singh DK, Luqman S. Lawsonia inermis (L.): A perspective on anticancer potential of Mehndi/Henna. *Biomed Res Ther*. 2014;**1**(18). https://doi.org/10.7603/s40730-014-0018-1.
27. Mamun AA, Zhao F. In-Plane Si Microneedles: Fabrication, Characterization, Modeling and Applications. *Micromachines*. 2022;**13**(5). [PubMed ID: 35630124]. [PubMed Central ID: PMC9146885]. https://doi.org/10.3390/mi13050657.
28. Erenoglu Sarı O, Donat R, Celik SS, Rajak DK. Micromolding-Based Fabrication of Dissolvable Microneedles: An Economical and Scalable Approach for Transdermal Drug Delivery. *Int J Polym Sci*. 2025;**2025**(1). https://doi.org/10.1155/ijps/2261987.
29. Chudzinska J, Wawrzynczak A, Feliczak-Guzik A. Microneedles Based on a Biodegradable Polymer-Hyaluronic Acid. *Polymers*. 2024;**16**(10). [PubMed ID: 38794589]. [PubMed Central ID: PMC11124840]. https://doi.org/10.3390/polym16101396.
30. Mohite P, Puri A, Munde S, Ade N, Kumar A, Jantrawut P, et al. Hydrogel-Forming Microneedles in the Management of Dermal Disorders Through a Non-Invasive Process: A Review. *Gels*. 2024;**10**(11). [PubMed ID: 39590075]. [PubMed Central ID: PMC11594199]. https://doi.org/10.3390/gels10110719.
31. Szpisjak-Gulyas N, Al-Tayawi AN, Horvath ZH, Laszlo Z, Kertesz S, Hodur C. Methods for experimental design, central composite design and the Box–Behnken design, to optimise operational parameters: A review. *Acta Alimentaria*. 2023;**52**(4):521-37. https://doi.org/10.1556/066.2023.00235.
32. Yan Q, Shen S, Wang Y, Weng J, Wan A, Yang G, et al. The Finite Element Analysis Research on Microneedle Design Strategy and Transdermal Drug Delivery System. *Pharmaceutics*. 2022;**14**(8). [PubMed ID: 36015251]. [PubMed Central ID: PMC9413279]. https://doi.org/10.3390/pharmaceutics14081625.
33. Tang X, Qin H, Zhang X, Yang H, Yang J, Chen P, et al. Design, optimization, and evaluation for a long-time-released transdermal microneedle delivery system containing estradiol. *Drug Deliv Transl Res*. 2024;**14**(6):1551-66. [PubMed ID: 38062287]. https://doi.org/10.1007/s13346-023-01471-z.
34. Tamez-Tamez JI, Vazquez-Lepe E, Rodriguez CA, Martinez-Lopez J, García-Lopez E. Assessment of geometrical dimensions and puncture feasibility of microneedles manufactured by micromilling. *Int J Adv Manuf Technol*. 2023;**126**(11-12):4983-96. https://doi.org/10.1007/s00170-023-11467-1.
35. Choupani A, Bediz B, Elitas M. Localized and controlled antibiotic therapy via microneedles: A biomedical approach to antimicrobial resistance. *J Drug Deliv Sci Technol*. 2026;**115**(1). https://doi.org/10.1016/j.jddst.2025.107639.
36. Nasiri MI, Vora LK, Ershaid JA, Peng K, Tekko IA, Donnelly RF. Nanoemulsion-based dissolving microneedle arrays for enhanced intradermal and transdermal delivery. *Drug Deliv Transl Res*. 2022;**12**(4):881-96. [PubMed ID: 34939170]. [PubMed Central ID: PMC8694761]. https://doi.org/10.1007/s13346-021-01107-0.
37. Ripolin A, Quinn J, Larraneta E, Vicente-Perez EM, Barry J, Donnelly RF. Successful application of large microneedle patches by human volunteers. *Int J Pharm*. 2017;**521**(1-2):92-101. [PubMed ID: 28216463]. [PubMed Central ID: PMC5364775]. https://doi.org/10.1016/j.ijpharm.2017.02.011.
38. Gomaa YA, Morrow DI, Garland MJ, Donnelly RF, El-Khordagui LK, Meidan VM. Effects of microneedle length, density, insertion time and multiple applications on human skin barrier function: assessments by transepidermal water loss. *Toxicol In Vitro*. 2010;**24**(7):1971-8. [PubMed ID: 20732409]. https://doi.org/10.1016/j.tiv.2010.08.012.
39. Klotz T, Ibrahim A, Maddern G, Caplash Y, Wagstaff M. Devices measuring transepidermal water loss: A systematic review of measurement properties. *Skin Res Technol*. 2022;**28**(4):497-539. [PubMed ID: 35411958]. [PubMed Central ID: PMC9907714]. https://doi.org/10.1111/srt.13159.
40. Naito C, Katsumi H, Suzuki T, Quan YS, Kamiyama F, Sakane T, et al. Self-Dissolving Microneedle Arrays for Transdermal Absorption Enhancement of Human Parathyroid Hormone (1-34). *Pharmaceutics*. 2018;**10**(4). [PubMed ID: 30400376]. [PubMed Central ID: PMC6320955]. https://doi.org/10.3390/pharmaceutics10040215.
41. Faizi HS, Vora LK, Nasiri MI, Wu Y, Mishra D, Anjani QK, et al. Deferasirox Nanosuspension Loaded Dissolving Microneedles for Intradermal Delivery. *Pharmaceutics*. 2022;**14**(12). [PubMed ID: 36559310]. [PubMed Central ID: PMC9784557]. https://doi.org/10.3390/pharmaceutics14122817.
42. Makoye A, Pogrebnoi A, Pogrebnaya T. Lawsone isomers, lawsone ether and bilawsone for dye-sensitized solar cells applications: DFT and UV-Vis studies. *J Mol Graph Model*. 2020;**94**:107457. [PubMed ID: 31586755]. https://doi.org/10.1016/j.jmgm.2019.107457.
43. Karimi A, Navidbakhsh M. Material properties in unconfined compression of gelatin hydrogel for skin tissue engineering applications. *Biomed Eng*. 2014;**59**(6). https://doi.org/10.1515/bmt-2014-0028.
44. Nguyen HX, Kipping T, Banga AK. Enhancement of Transdermal Drug Delivery: Integrating Microneedles with Biodegradable Microparticles. *Mol Pharm*. 2025;**22**(2):984-1009. [PubMed ID: 39823349]. https://doi.org/10.1021/acs.molpharmaceut.4c01202.
45. Costa P, Sousa Lobo JM. Modeling and comparison of dissolution profiles. *Eur J Pharm Sci*. 2001;**13**(2):123-33. [PubMed ID: 11297896]. https://doi.org/10.1016/s0928-0987(01)00095-1.

46. Nadeem AY, Ul Islam M, Khan S, Al-Suhaimi EA, Shehzad A, Noor A. Transdermal glucose responsive composite polymeric microneedle patches for personalized diabetes treatment: A novel approach to precision medicine. *J Drug Deliv Sci Technol*. 2025;**111**. https://doi.org/10.1016/j.jddst.2025.107161.
47. Khairnar P, Phatale V, Shukla S, Tijani AO, Hedaoo A, Strauss J, et al. Nanocarrier-Integrated Microneedles: Divulging the Potential of Novel Frontiers for Fostering the Management of Skin Ailments. *Mol Pharm*. 2024;**21**(5):2118-47. [PubMed ID: 38660711]. https://doi.org/10.1021/acs.molpharmaceut.4c00144.
48. Al-Japairai K, Almurisi SH, Alheibshy F, Abdul-Halim N, Mahmood S. Rapid dissolving microneedle patch integrated with benidipine-loaded nanotransfersomes for transdermal drug delivery: optimization, characterizations, and preclinical bioavailability assessment. *Drug Deliv Transl Res*. 2025. [PubMed ID: 41094229]. https://doi.org/10.1007/s13346-025-01976-9.
49. Khan B, Kraisit P, Santhan S, Hirun N. Box-Behnken Design Assisted Optimization and Characterization of Chitosan Film for Simultaneous Topical Delivery of Ascorbic Acid and Metronidazole. *Pharmaceutics*. 2025;**17**(5). [PubMed ID: 40430855]. [PubMed Central ID: PMC12115047]. https://doi.org/10.3390/pharmaceutics17050562.
50. Cammarano A, Dello Iacono S, Meglio C, Nicolais L. Advances in Transdermal Drug Delivery Systems: A Bibliometric and Patent Analysis. *Pharmaceutics*. 2023;**15**(12). [PubMed ID: 38140102]. [PubMed Central ID: PMC10747220]. https://doi.org/10.3390/pharmaceutics15122762.
51. Wang X, Wang Z, Xiao M, Li Z, Zhu Z. Advances in biomedical systems based on microneedles: design, fabrication, and application. *Biomater Sci*. 2024;**12**(3):530-63. [PubMed ID: 37971423]. https://doi.org/10.1039/d3bm01551c.
52. Liu T, Luo G, Xing M. Biomedical Applications of Polymeric Microneedles for Transdermal Therapeutic Delivery and Diagnosis: Current Status and Future Perspectives. *Adv Ther*. 2020;**3**(9). https://doi.org/10.1002/adtp.201900140.
53. Lee JY, Dong SH, Ng KW, Goh CF. Assessing the integrity and mechanical properties of commercial microneedles: innovation or fad? *Drug Deliv Transl Res*. 2025;**15**(11):3986-4003. [PubMed ID: 40450125]. [PubMed Central ID: PMC12507953]. https://doi.org/10.1007/s13346-025-01888-8.
54. Yolai N, Shu W, O'cearbhaill ED, Modchang C, Annaidh AN. Finite element analysis of polymeric microneedle insertion into skin. *Mater Des*. 2025;**259**. https://doi.org/10.1016/j.matdes.2025.114936.
55. Tsuboko Y, Sakoda H, Okamoto Y, Nomura Y, Yamamoto E. Mechanical Characterization of Individual Needles in Microneedle Arrays: Factors Affecting Compression Test Results. *Pharmaceutics*. 2024;**16**(11). [PubMed ID: 39598602]. [PubMed Central ID: PMC11597646]. https://doi.org/10.3390/pharmaceutics16111480.
56. Mangang KN, Thakran P, Halder J, Yadav KS, Ghosh G, Pradhan D, et al. PVP-microneedle array for drug delivery: mechanical insight, biodegradation, and recent advances. *J Biomater Sci Polym Ed*. 2023;**34**(7):986-1017. [PubMed ID: 36541167]. https://doi.org/10.1080/09205063.2022.2155778.
57. Siepmann J, Peppas NA. Higuchi equation: derivation, applications, use and misuse. *Int J Pharm*. 2011;**418**(1):6-12. [PubMed ID: 21458553]. https://doi.org/10.1016/j.ijpharm.2011.03.051.
58. Wang B, Liao L, Liang H, Chen J, Qiu Y. Preparation and In Vitro/In Vivo Characterization of Mixed-Micelles-Loaded Dissolving Microneedles for Sustained Release of Indomethacin. *Pharmaceutics*. 2024;**16**(12). [PubMed ID: 39771485]. [PubMed Central ID: PMC11728531]. https://doi.org/10.3390/pharmaceutics16121505.
59. Batiha GE, Teibo JO, Shaheen HM, Babalola BA, Teibo TKA, Al-Kuraishy HM, et al. Therapeutic potential of Lawsonia inermis Linn: a comprehensive overview. *Naunyn Schmiedebergs Arch Pharmacol*. 2024;**397**(6):3525-40. [PubMed ID: 38010396]. [PubMed Central ID: PMC11111528]. https://doi.org/10.1007/s00210-023-02735-8.
60. Meng F, Qiao X, Xin C, Ju X, He M. Recent progress of polymeric microneedle-assisted long-acting transdermal drug delivery. *J Pharm Pharm Sci*. 2024;**27**:12434. [PubMed ID: 38571937]. [PubMed Central ID: PMC10987780]. https://doi.org/10.3389/jpps.2024.12434.